CaM kinase II initiates meiotic spindle depolymerization independently of APC/C activation

Simone Reber,[1] Sabine Over,[1] Iva Kronja,[2] and Oliver J. Gruss[1]

[1]Zentrum für Molekulare Biologie der Universität Heidelberg, Deutsches Krebsforschungszentrum und Zentrum für Molekulare Biologie Heidelberg Allianz (DKFZ-ZMBH Alliance), 69120 Heidelberg, Germany
[2]Cell Biology and Biophysics Program, European Molecular Biology Laboratory, 69126 Heidelberg, Germany

Altered spindle microtubule dynamics at anaphase onset are the basis for chromosome segregation. In *Xenopus laevis* egg extracts, increasing free calcium levels and subsequently rising calcium-calmodulin–dependent kinase II (CaMKII) activity promote a release from meiosis II arrest and reentry into anaphase. CaMKII induces the activation of the anaphase-promoting complex/cyclosome (APC/C), which destines securin and cyclin B for degradation to allow chromosome separation and mitotic exit.

In this study, we investigated the calcium-dependent signal responsible for microtubule depolymerization at anaphase onset after release from meiotic arrest in *Xenopus* egg extracts. Using Ran–guanosine triphosphate–mediated microtubule assemblies and quantitative analysis of complete spindles, we demonstrate that CaMKII triggers anaphase microtubule depolymerization. A CaMKII-induced twofold increase in microtubule catastrophe rates can explain reduced microtubule stability. However, calcium or constitutively active CaMKII promotes microtubule destabilization even upon APC/C inhibition and in the presence of high cyclin-dependent kinase 1 activity. Therefore, our data demonstrate that CaMKII turns on parallel pathways to activate the APC/C and to induce microtubule depolymerization at meiotic anaphase onset.

Introduction

Faithful chromosome segregation to both daughter cells is essential for stable inheritance of genetic material and depends on proper function of the M-phase spindle. Spindle microtubules capture and coordinately align all chromosomes into a common plane in metaphase via interactions with kinetochores and chromosome arms. They further exert the mechanical forces that mediate synchronous segregation of sister chromatids to the spindle poles in anaphase. To cope with these functions during M phase, the general parameters determining microtubule dynamics not only change early in M phase but also at the onset of anaphase concomitant with chromosome segregation (Verde et al., 1990; for reviews see Compton, 2000; Mitchison and Salmon, 2001; Wittmann et al., 2001; Cassimeris and Skibbens, 2003; Gadde and Heald, 2004; Kline-Smith and Walczak, 2004).

At the molecular level, anaphase onset is defined by the activation of the anaphase-promoting complex/cyclosome (APC/C), a multisubunit E3 ubiquitin ligase that destines securin/Pds1 and mitotic cyclins for degradation. Degradation of securin is required for the activation of separase. Active separase cleaves the SCC1 subunit of the cohesin complex, which mediates chromatid cohesion until anaphase onset (Nasmyth, 2002; Yanagida, 2005).

In contrast, the molecular mechanisms, which induce the changes in microtubule behavior at the beginning of anaphase, are less well understood. Changes in microtubule dynamics in early M phase are governed by an increase in the activity of Cdk1, the general regulator of M phase (Verde et al., 1990). Cdk1 is activated in the presence of rising levels of M-phase cyclins and modulates the activity of a variety of microtubule-associated proteins (MAPs) and motor proteins (Cassimeris and Spittle, 2001). In turn, degradation of M-phase cyclins and thus declining Cdk1 activity upon activation of the APC/C are assumed to determine changes in microtubule behavior at the onset of anaphase.

S. Reber and S. Over contributed equally to this paper.

Correspondence to Oliver J. Gruss: o.gruss@zmbh.uni-heidelberg.de

Abbreviations used in this paper: APC/C, anaphase-promoting complex/cyclosome; CaMKII, calcium-calmodulin–dependent kinase II; CSF, cytostatic factor; MAP, microtubule-associated protein; XErp, *Xenopus* Emi1-related protein.

The Rockefeller University Press $30.00
J. Cell Biol. Vol. 183 No. 6 1007–1017
www.jcb.org/cgi/doi/10.1083/jcb.200807006

Spindle assembly, chromosome segregation, and spindle depolymerization in anaphase can be recapitulated in the cell-free system of *Xenopus laevis* egg extracts (Murray, 1991; Sawin and Mitchison, 1991; Holloway et al., 1993). M-phase extracts assemble astral arrays of microtubules from purified human centrosomes (Tournier et al., 1991), meiotic spindles around chromatin beads (Heald et al., 1996), and complete bipolar spindles from sperm nuclei (Sawin and Mitchison, 1991). Moreover, the addition of GTP-locked Ran, e.g., of the hydrolysis-deficient mutant RanQ69L, is sufficient to induce the formation of microtubule assemblies in *Xenopus* M-phase extracts (Carazo-Salas et al., 1999). Assaying Ran-GTP–induced microtubule assembly has been successfully used to analyze molecular details about M-phase spindle assembly pathways (Clarke and Zhang, 2004; Gruss and Vernos, 2004; Ciciarello et al., 2007).

Like intact unfertilized vertebrate eggs, *Xenopus* M-phase egg extracts are held in metaphase by the activity of the cytostatic factor (CSF), the central activity of which is the *Xenopus* Emi1-related protein (XErp). XErp largely inhibits the APC/C-dependent cyclin destruction and consequently maintains high Cdk1 activity (Schmidt et al., 2005; Tung et al., 2005). Upon fertilization, reentry into the cell cycle is triggered by a transient increase in free intracellular calcium (Busa and Nuccitelli, 1985). In the cell-free system, the direct addition of calcium likewise mimicks fertilization (Murray, 1991). In both intact eggs and cell-free egg extracts, calcium-activated calcium-calmodulin–dependent kinase II (CaMKII) directly phosphorylates XErp. Phosphorylation-dependent degradation of XErp eventually leads to the activation of APC/C and, in turn, to the degradation of cyclin B and securin, inducing anaphase onset (Liu and Maller, 2005; Rauh et al., 2005; Hansen et al., 2006).

At the same time, the stability of spindle microtubules changes significantly in the *Xenopus* system. Both kinetochore and nonkinetochore microtubules apparently shorten from their plus ends, which results in an overall decrease in microtubule density in the central part of the spindle (Holloway et al., 1993; Murray et al., 1996; Desai et al., 1998; Maddox et al., 2003). The characteristic reduction in spindle microtubule density upon induction of anaphase is also observed in the presence of nondegradable mitotic cyclin (cyclinBΔ90) at concentrations that allow chromosome segregation but avoid mitotic exit (Holloway et al., 1993; Murray et al., 1996). However, more recent experiments show that high Cdk1 activity blocks sister chromatid separation even upon activation of APC/C and securin degradation (Stemmann et al., 2001). Therefore, the previous data are consistent with the idea that a partial reduction of the metaphase Cdk1 activity might be responsible for the observed changes in microtubule stability in anaphase.

In this study, we systematically investigate the role of APC/C activation and the reduction in Cdk1 activities on changes in microtubule stability in anaphase of *Xenopus* egg extracts. Our data indicate that there is a general decrease in microtubule stability in meiotic anaphase, which can be recapitulated in complete spindles, centrosomally or chromatin-nucleated microtubules, as well as in Ran-GTP–mediated microtubule assemblies. The general reduction in microtubule stability is marked by a twofold increase in microtubule catastrophe rates. We show that high Cdk1 levels cannot rescue microtubule stability after induction of anaphase. Moreover, neither the degradation of cyclin B nor the activation of APC/C is required for microtubule destabilization. However, the addition of free calcium or constitutively active purified CaMKII still leads to the destabilization of microtubules. Strikingly, constitutively active CaMKII disassembles spindles even in the presence of the APC/C inhibitor XErp and thus stable securin and cyclin B. Our data demonstrate the existence of a novel CaMKII-dependent mechanism that initiates the destabilization of spindle microtubules in CSF-arrested *Xenopus* egg extracts parallel to APC/C activation at the metaphase to anaphase transition.

Results

To investigate changes in microtubule stability from metaphase to anaphase, we assembled spindles from sperm nuclei in CSF-arrested *Xenopus* egg extracts supplemented with Cy3-labeled tubulin. We initiated anaphase by adding 0.6 mM calcium but blocked cell cycle progression in anaphase using nondegradable cyclin B (cyclinBΔ90) to maintain high Cdk1 activity throughout the experiment (Fig. 1 A). After the addition of calcium and thus anaphase initiation, the density of spindle microtubules in the central part of the spindle was decreased concomitant with chromosome segregation, but spindles did not completely depolymerize (Fig. 1 B, top right). Like sperm nuclei, Ran-GTP and chromatin beads readily assembled microtubule structures in CSF-arrested *Xenopus* egg extracts (Fig. 1 B, left). In contrast, neither Ran-GTP nor chromatin beads stabilized any microtubules in anaphase extracts in the presence of cyclinBΔ90, suggesting an overall reduced microtubule stability (Fig. 1 B, right).

It is known that Ran-GTP produced by nuclei or chromatin beads releases the MAP TPX2 and other MAPs from importins. Only free TPX2 induces microtubule assembly and interacts with and activates aurora A/Eg2 (Gruss and Vernos, 2004). To address the efficiency of TPX2 release from importins in the presence of Ran-GTP in metaphase and anaphase, we compared the amounts of Eg2 associated with free TPX2 after the addition of RanQ69L (Fig. 1 C). Eg2 was efficiently coprecipitated on TPX2 antibodies both in metaphase and anaphase (Fig. 1 C). This shows that a decrease in microtubule stability in anaphase is not caused by an inefficient release of TPX2 from importins but might reflect a general feature of *Xenopus* extracts in anaphase. To confirm this, we extended our analysis to microtubules assembled from purified human centrosomes, which promote microtubule assembly independently of Ran-GTP (Fig. 1 D; Carazo-Salas et al., 1999). Like Ran-GTP or chromatin beads, centrosomes did not induce de novo microtubule assembly in anaphase (Fig. 1 D, middle). Also, astral arrays that preformed around purified human centrosomes in metaphase (Fig. 1 D, left) quickly depolymerized in anaphase (Fig. 1 D, right). These data suggest a global regulation of microtubule stability at the transition from metaphase to anaphase in *Xenopus* egg extracts.

A possible explanation for our observations is that activation of the APC/C, degradation of cyclin B, and a following drop in Cdk1 activity led to a changed phosphorylation pattern of MAPs and motors and consequently to the destabilization of

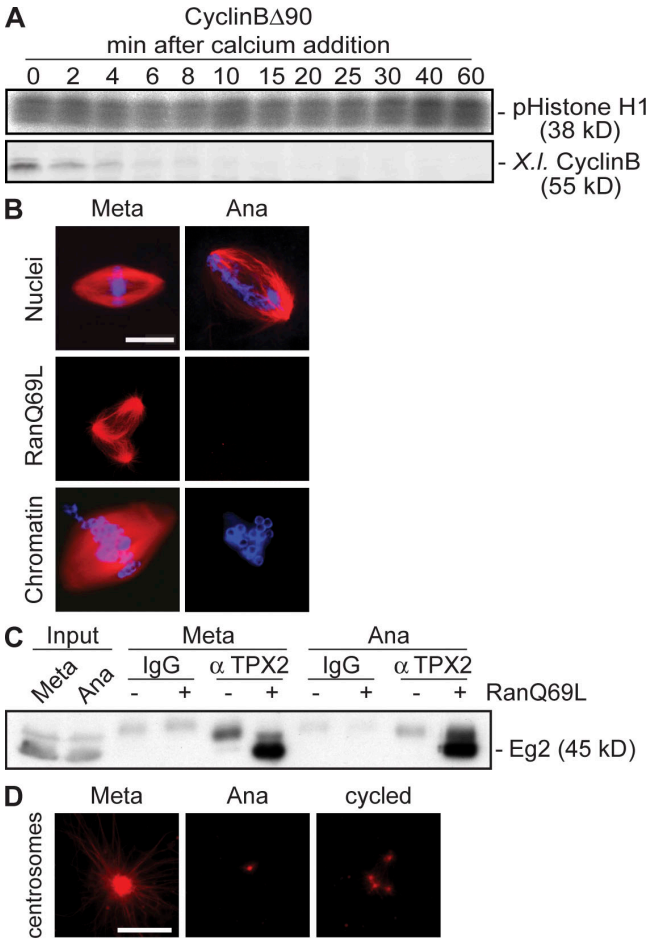

Figure 1. **Changes in microtubule stability from metaphase to anaphase in *Xenopus* egg extracts.** (A) Calcium was added to CSF-arrested *Xenopus* egg extracts (0 min) in the presence of cyclinBΔ90, and samples were withdrawn at the indicated times to determine the activity of Cdk1 toward histone H1 (pHistone H1, top) and the amounts of endogenous cyclin B (*X.I. cyclin B*, bottom). (B) Microtubules or spindles were assembled in metaphase-arrested extracts (left), calcium was added in the presence of cyclinBΔ90 (right), and microtubules were visualized by direct fluorescence of added Cy3-tubulin. Sperm nuclei, RanQ69L, or chromatin beads were used as a nucleating source. (C) Immunoprecipitation using anti-TPX2 antibodies from metaphase or anaphase extracts. Immunocomplexes were eluted with high salt, and aurora A/Eg2 was determined by immunoblotting. (D) The microtubule assembly assay is as described in B; purified human centrosomes were used as a nucleating source. Cycled, microtubule asters were preassembled in metaphase before calcium addition; Meta, metaphase; Ana, anaphase. Bars, 10 μm.

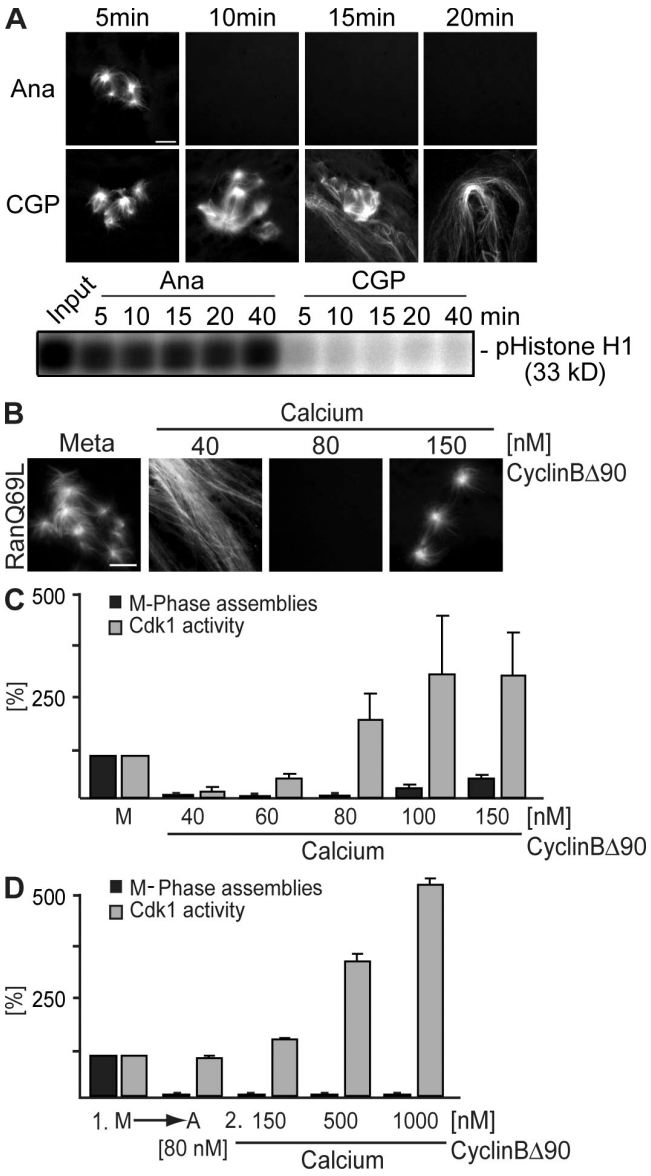

Figure 2. **Correlation of Cdk1 activity and changes in microtubule stability at metaphase to anaphase transition.** (A) CSF-arrested egg extracts were incubated with calcium and cyclinBΔ90 (Ana) or CGP74514A (CGP). Ran-GTP–mediated microtubule assemblies were visualized by direct fluorescence after the addition of Cy3-labeled tubulin (top), and Cdk1 activities were determined by a histone H1 kinase activity assay (bottom). (B–D) CSF-arrested egg extracts (Meta or M) were triggered to go into anaphase by calcium addition in the presence of increasing cyclinBΔ90 concentrations. Ran-GTP–induced metaphase microtubule assemblies were visualized (B) and quantified relative to metaphase as indicated (C, black bars). In parallel, the Cdk1 kinase activity was measured using histone H1 phosphorylation (C, gray bars). (D) Anaphase was first induced with calcium in the presence of 80 nM cyclinBΔ90, increasing amounts of cyclinBΔ90 were added, and the capacity of Ran-GTP to still induce microtubule assembly was tested. These assemblies were quantified relative to metaphase (black bars), and the Cdk1 kinase activity was measured using histone H1 phosphorylation (gray bars). Error bars represent SD from three independent experiments. Ana, anaphase; Meta, metaphase. Bars, 5 μm.

microtubules. To test this, we assembled microtubule structures by the addition of Ran-GTP and subsequently observed their stability upon Cdk1 inhibition using CGP74514A (CGP), a selective chemical inhibitor of Cdk1 kinase (Fig. 2 A; Skoufias et al., 2007). Surprisingly, Ran-induced structures did not disassemble upon Cdk1 inhibition before interphasic microtubules were detectable (Fig. 2 A, CGP; see 15 min for coexisting M phase and interphase microtubule structures). In contrast, metaphase microtubule structures disassembled as expected upon the addition of calcium (Fig. 2 A, top) despite high Cdk1 activity (Fig. 2 A, bottom; Ana). This suggested that the sole reduction of Cdk1 activity is not sufficient for the observed changes in anaphase microtubule stability. To analyze the correlation between Cdk1 activity and microtubule stability more quantitatively, we determined Ran-GTP–mediated microtubule assemblies at different concentrations of nondegradable cyclin B. When cylinBΔ90 was added to only 40 nM and anaphase onset was induced by calcium addition, the system exited mitosis as judged

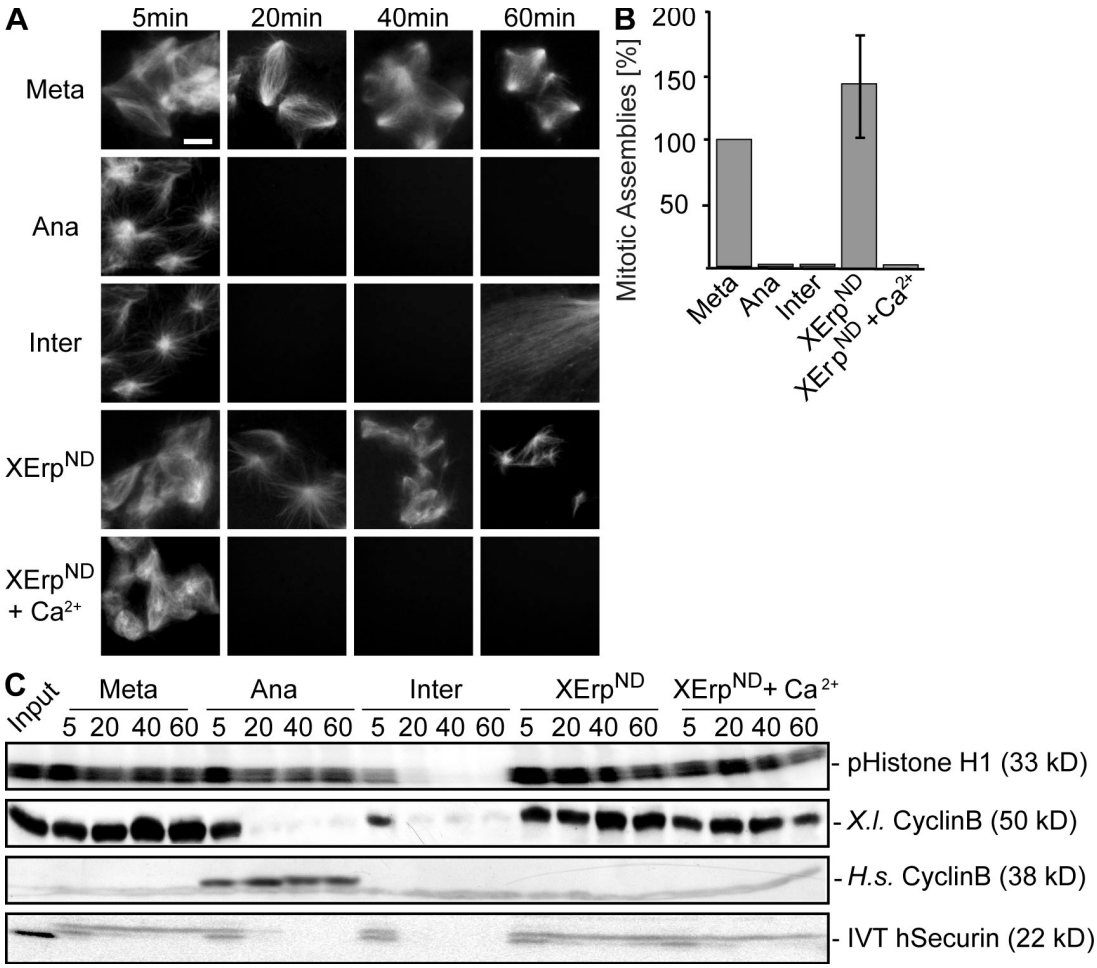

Figure 3. **APC/C activation is not required for changes in microtubule stability.** (A) CSF extracts containing Cy3-tubulin and in vitro translated exogenously added securin were preincubated for 10 min in the presence of Ran-GTP to preassemble microtubules. Reactions were treated with buffer (Meta), calcium and cyclinBΔ90 (Ana), calcium (Inter), $XErp^{ND}$, or calcium and $XErp^{ND}$ ($XErp^{ND}$ + Ca^{2+}). Microtubule structures were visualized by direct fluorescence of Cy3-tubulin. (B) Quantification of microtubule assemblies counted at the 40-min time point imaged in A. Error bars represent SD from three independent experiments; metaphase was set to 100%. (C) Amounts of cyclin B (endogenous, *X.l.* cyclin B; exogenously added [Δ90], *H.s.* cyclin B) were determined by immunoblotting, and amounts of exogenously added in vitro translated (IVT) securin were determined by autoradiography; Cdk1 activities were measured by histone H1 phosphorylation (pHistone H1). Meta, metaphase; Ana, anaphase; Inter, interphase. Bar, 5 µm.

by long and stable interphasic microtubules. Upon the addition of cyclinBΔ90 to endogenous levels (80 nM; Stemmann et al., 2001), no microtubule structures were observed (Fig. 1). This indicates that anaphase is faithfully established and maintained upon calcium addition and physiological cyclinBΔ90 levels. The addition of >150 nM cyclinBΔ90 allowed some but still significantly less microtubule assemblies than in metaphase (Fig. 2, B and C). Moreover, no microtubule assembly was observed if anaphase was initially established at 80 nM cyclinBΔ90, and the concentration only subsequently increased even up to 1 µM (Fig. 2 D).

These results suggested three conclusions: first, metaphase Cdk1 activity allows microtubule destabilization in meiotic anaphase, and inhibition of this activity alone does not promote microtubule destabilization. Second, elevated Cdk1 activity can partially rescue microtubule stability at anaphase onset, but, third, after anaphase induction at metaphase Cdk1 activity, the transition to less stable microtubules becomes resistant to high Cdk1 activity. These conclusions contradict the simple model that calcium and CaMKII activate only the APC/C in meiotic anaphase, which destines cyclin B for degradation leading to decreased Cdk1 activity and thus causes anaphase microtubule destabilization.

As cyclin B degradation is mediated by APC/C activity (but according to our experiments is not required to destabilize microtubules), we aimed to further determine the overall role of APC/C activation in changing microtubule stability in anaphase. We assayed Ran-GTP–induced microtubule assembly by direct fluorescence and monitored cyclin B and securin levels as well as Cdk1 activity to determine APC/C activation in metaphase, anaphase, and interphase. To inhibit APC/C activation despite calcium-induced anaphase onset and therefore uncoupling APC/C activation from other calcium-dependent processes, we used a nondegradable variant of XErp ($XErp^{ND}$; Fig. 3; Rauh et al., 2005). As expected, Ran-GTP–induced microtubule assemblies were stable in CSF-arrested extracts, and high levels of cyclin B, securin, and Cdk1 activity were maintained (Fig. 3, A–C; Meta). Calcium induced the destabilization of microtubule

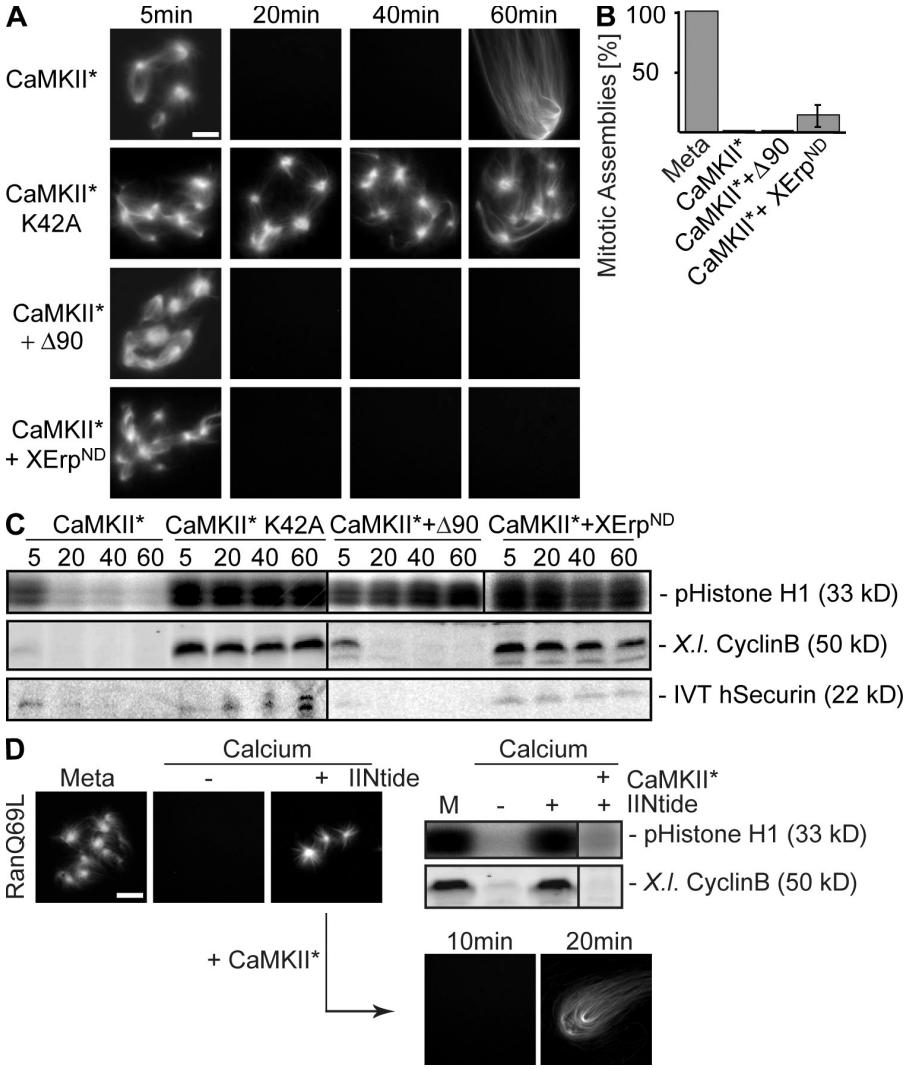

Figure 4. **CaMKII induces microtubule instability in anaphase.** CSF extracts containing Cy3-tubulin and in vitro translated securin were preincubated for 10 min in the presence of RanQ69L to preassemble microtubules. (A) Reactions were treated with constitutively active CaMKII (CaMKII*), the catalytically inactive mutant (CaMKII*K42A), or CaMKII* together with cyclinBΔ90 (CaMKII* + Δ90) or $XErp^{ND}$ (CamKII* + $XErp^{ND}$) as indicated. Microtubule assemblies were visualized by direct fluorescence. (B) Quantification of microtubule assemblies counted in A after 40 min. Error bars represent SD from three independent experiments; metaphase was set to 100%. (C) Reactions were performed as in A; the amounts of endogenous cyclin B (*X.l.* cyclin B) were determined by immunoblotting, and the amounts of exogenously added in vitro translated (IVT) securin were determined by autoradiography; Cdk1 activities were measured by histone H1 phosphorylation (pHistone H1). (D) Inhibition of endogenous CaMKII activity; CSF extracts containing Cy3-tubulin and RanQ69L were left untreated (Meta) or incubated with calcium in the absence (−) or presence (+) of the CaMKII inhibitor IINtide. (left) Microtubule structures were visualized by direct fluorescence of Cy3-tubulin. (right) Cyclin B (*X.l.* cyclin B) and Cdk1 activity (pHistone H1) were determined. (D, bottom) Reactions were chased using CaMKII* for the indicated time points and were visualized. Bars, 5 μm.

assemblies as well as cyclin B and securin degradation, but high Cdk1 activity was maintained in the presence of cyclinBΔ90 (Fig. 3, A–C; Ana). Likewise, microtubule destabilization was observed in the absence of cyclinBΔ90 but was followed by mitotic exit (Fig. 3 A, Inter; note the appearance of interphasic microtubules after 60 min). Although $XErp^{ND}$ alone had no effect in metaphase (Fig. 3, A–C; $XErp^{ND}$), interestingly, it allowed microtubule disassembly upon calcium addition (Fig. 3, A and B; $XErp^{ND}$ + Ca^{2+}) despite efficient inhibition of APC/C activation as indicated by stable cyclin B and securin (Fig. 3 C, $XErp^{ND}$ + Ca^{2+}). These results strongly suggest that the depolymerization of microtubules in anaphase of *Xenopus* egg extracts is triggered by calcium but does not require the activation of APC/C and, therefore, the degradation of its metaphase substrates securin and cyclin B.

Increasing calcium levels and subsequent CaMKII activation initiate metaphase to anaphase transition in CSF-arrested egg extracts. This conclusion was initially based on the observation that constitutively active CaMKII promotes anaphase entry also in the absence of free calcium (Lorca et al., 1993). Therefore, we aimed to test the stability of Ran-GTP–induced microtubule assemblies after anaphase induction by constitutively active CaMKII (CaMKII 1–290 [Lorca et al., 1993] and CaMKII* [Fig. S1, available at http://www.jcb.org/cgi/content/full/jcb.200807006/DC1]). We recombinantly expressed and purified CaMKII*, and, as a control, a corresponding mutant in which a lysine in position 42 essential for nucleotide binding was replaced by an alanine (CaMKII*K42A; Hanks and Quinn, 1991). The mutant protein displayed no detectable activity on myelin basic protein, whereas the activity of the wild-type kinase could be readily detected and quantified (see Materials and methods and Fig. S1). When added to *Xenopus* egg extract, CaMKII* triggered the destabilization of preassembled microtubule structures and promoted entry into interphase as judged by typically long interphasic microtubules (Fig. 4, A and B; CaMKII*). Consistent with this, it induced the degradation of endogenous cyclin B (Fig. 4 C, *X.l.* cyclin B) and securin as well as decreased Cdk1 activities (Fig. 4 C, CaMKII*). In contrast, the mutant kinase had no effect on the system (Fig. 4, A and C; CaMKII*K42A). Microtubules were also destabilized by CaMKII*-induced anaphase entry in the presence of cyclinBΔ90 (Fig. 4, A and B; CaMKII* + Δ90), which rescued high Cdk1 activity, although APC/C was activated (Fig. 4 C, CaMKII* + Δ90; see degradation of endogenous securin and cyclin B). Likewise, inhibition of

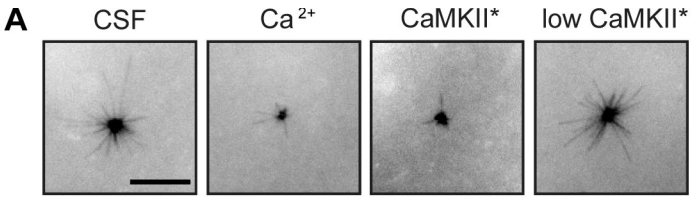

B

	CSF	Calcium		CaMKII*		low CaMKII*	
		0-15 min	15-25 min	0-15 min	15-25 min	0-15 min	15-25 min
MT [n]	64	55	84	60	60	47	45
Time [s]	2828	1084	2334	1590	1368	1570	1858
vg [µm/min]	12.2 ±12.9	11.2 ±8.6	26.9 ±17.2	12.2 ±10.3	17.0 ±12.4	29.1 ±25.1	14.8 ±9.7
vs [µm/min]	21.0 ±15	17.5 ±12.2	23.3 ±14.2	17.0 ±9.7	20.1 ±13.7	25.9 ±23.7	15.8 ±11.3
fcat [min^{-1}]	2.94	5.52	4.50	5.16	5.94	3.06	3.66
fres [min^{-1}]	0.20	0	0.30	0.30	0.06	0.36	0

Figure 5. **Dynamic measurements of centrosomally nucleated microtubules in metaphase or anaphase.** CSF-arrested egg extracts were supplemented with Cy3-tubulin and purified human centrosomes and were triggered to enter anaphase as indicated. (A) Microtubules were visualized by time-lapse microscopy in 2-s intervals, and microtubules were tracked manually. Still images (after 15 min) are shown. (B) Parameters of dynamic instability were determined from data gained by time-lapse imaging using a Matlab macro. MT, microtubules; vg, growth rate; vs, shrinkage rate; fcat, catastrophe frequency; fres, rescue frequency. Bar, 10 µm.

APC/C activation by XErpND (Fig. 4 C, CaMKII* + XErpND; note that cyclin B and securin are stable) did not interfere with the CaMKII*-induced reduction in microtubule stability (Fig. 4, A and B; CaMKII* + XErpND).

To judge whether the level of added CaMKII* was comparable with the physiological calcium-induced CaMKII activity, we compared phosphorylation of the CaMKII substrate autocamtide-2 (Jones and Persaud, 1998) in egg extracts upon calcium or CaMKII* addition. Within a few minutes after the addition of calcium, a transient increase in substrate phosphorylation was observed, whereas hardly any substrate phosphorylation could be detected in untreated CSF-arrested extracts (Fig. S1, −3 time points). In comparison, purified CaMKII* added to egg extracts phosphorylated autocamtide-2 with a very similar efficiency as endogenous CaMKII, whereas the activity of the same amount of the K42A mutant was undetectable in extracts (Fig. S1). Lower concentrations of CaMKII* activity resulted in less efficient substrate phosphorylation (Fig. S1, low CaMKII*). Interestingly, the addition of lower CaMKII* activity to metaphase egg extracts still led to APC/C activation in the absence or presence of cyclinBΔ90 but was insufficient to efficiently promote microtubule destabilization (Fig. S2, available at http://www.jcb.org/cgi/content/full/jcb.200807006/DC1). The latter data suggest independent mechanisms for microtubule depolymerization and APC/C activation. Collectively, our experiments support the conclusion that microtubule destabilization at anaphase onset after release from CSF arrest can be induced by constitutively active CaMKII and occurs independently of APC/C activation.

The observation of CaMKII*-induced microtubule depolymerization suggested that endogenous CaMKII activity would be required for calcium-induced microtubule destabilization. Therefore, we assayed the stability of metaphase microtubule assemblies (Fig. 4 D, Meta) after calcium addition in the absence or presence of a CaMKII inhibitor, which corresponds to the N-terminal inhibitory domain of CaMKII (IINtide; Chang et al., 2001). As expected, no M-phase microtubules were found after anaphase induction in the absence of the inhibitor (Fig. 4 D, calcium − IINtide), cyclin B was degraded, and the Cdk1 activity was reduced (Fig. 4 D, right; calcium − IINtide). In contrast, Ran-GTP–induced microtubule assemblies could be readily observed in the presence of IINtide despite calcium addition (Fig. 4 D, left; calcium + IINtide). Cyclin B stayed stable, and the Cdk1 activity remained high (Fig. 4 D, right; calcium + IINtide). Still, the addition of constitutively active CaMKII* induced both APC/C activation and microtubule destabilization even in the presence of the inhibitor (Fig. 4 D, right; + CaMKII* + IINtide and bottom), indicating that its inhibitory effect is specific for CaMKII. Moreover, IINtide efficiently inhibited calcium-dependent phosphorylation of autocamtide-2 in egg extracts (Fig. S1). Similar results were seen using another CaMKII inhibitor peptide (CaMKII$_{281–309}$) as well as a general calmodulin inhibitor (Lorca et al., 1993; Morin et al., 1994), whereas the addition of cyclosporin A to prevent activation of the calcium-calmodulin–dependent phosphatase calcineurin had no effect on microtubule depolymerization (Fig. S3, available at http://www.jcb.org/cgi/content/full/jcb.200807006/DC1). These results show that calcium-induced depolymerization of microtubules in anaphase of *Xenopus* egg extracts requires the activation of CaMKII.

The apparent changes in the stability of the aforementioned microtubules were likely caused by changes in dynamic instability parameters from metaphase to anaphase in the *Xenopus* system. To visualize and quantify these changes, we assembled Cy3-labeled microtubules from centrosomes and tracked them by time-lapse microscopy in metaphase or anaphase extracts (Fig. 5). It is known that in *Xenopus* metaphase extracts, the relatively short mean length of microtubules is largely determined by their high catastrophe frequency, which elevates at the entry into M phase to two to three catastrophes per minute (Niethammer et al., 2007). Consistent with that, microtubules in

CSF-arrested extracts in our hands showed catastrophes with a frequency of 2.94 min^{-1} (Fig. 5, A and B; and Video 1, available at http://www.jcb.org/cgi/content/full/jcb.200807006/DC1).

The addition of calcium specifically induced an elevation of the catastrophe frequency to 5.52 and 4.50 min^{-1} in two time intervals measured (Fig. 5, A and B; and Video 2, available at http://www.jcb.org/cgi/content/full/jcb.200807006/DC1) but did not consistently influence growth or shrinkage rates. Similar to metaphase, microtubules after induction of anaphase by low CaMKII* activity consistently underwent catastrophes at a frequency of 3.06 or 3.66 min^{-1} (Fig. 5, A and B; and Video 3). In contrast, the addition of physiological doses of CaMKII* increased the catastrophe frequency to 5.16 and 5.94 min^{-1}, whereas growth and shrinkage rates and rescue frequencies were not significantly changed (Fig. 5, A and B; and Video 4). These numbers are in striking agreement with the catastrophe frequencies measured after anaphase induction with calcium. Although microtubule dynamics measurements usually vary between different *Xenopus* extract preparations in absolute numbers, the approximately twofold relative changes in catastrophe frequency could reproducibly be observed (see Fig. S4 for a second independent dataset). Therefore, we conclude that reduced microtubule stability in meiotic anaphase can be at least in part explained by a twofold increase in microtubule catastrophe rates from metaphase to anaphase induced by activated CaMKII.

Our experiments on Ran-GTP–induced microtubule assemblies and centrosomal asters suggested a novel CaMKII-induced mechanism for anaphase microtubule destabilization. Therefore, we intended to analyze microtubule stability at the metaphase to anaphase transition in complete bipolar spindles assembled around sperm nuclei in *Xenopus* egg extracts. We visualized and quantified spindle microtubule densities by direct fluorescence of Cy3-labeled tubulin before and after anaphase onset by calcium or CaMKII*. For each condition, we imaged 40–80 spindle structures. Within all acquired images, the two poles were defined manually, and the mean fluorescence was determined using ImageJ to assay for the overall microtubule stability of the spindles (Fig. 6 A, intensity). A custom Matlab macro vertically aligned the spindles along the pole to pole axis, determined the mean pole to pole distance as a measure for spindle size (Fig. 6 A), and subsequently rescaled all spindles to the same size. Matlab was used to quantify and plot the fluorescence (i.e., microtubule) intensity distributions in a 1.5-µm-wide area along the pole to pole axis (Fig. 6 A, blue line). Metaphase spindles typically showed aligned chromosomes and a high local microtubule density in the central part close to the chromosomes (Fig. 6 A, Meta). Entry into anaphase after calcium addition led to a reduction of the intensity (33%) and to a slight (21%) decrease in spindle size (pole to pole distance; Fig. 6 A, calcium). Anaphase onset triggered by CaMKII* promoted a two-third decrease in intensity and an almost twofold reduction of spindle size as compared with metaphase (Fig. 6 A, CaMKII*). CaMKII-induced depolymerization was therefore more efficient than what was observed upon the addition of calcium (Fig. 6 A, CaMKII* and calcium; see average and intensity). However, under either condition we observed a characteristic local decrease in microtubule density in the central part of the spindle, which is consistent with previously published data on anaphase spindles (Murray et al., 1996). Calcium or CaMKII* addition led to the quick degradation of securin and cyclin B and reduced Cdk1 activity (Fig. 6 B). Importantly, the CaMKII*-induced reduction in spindle size and the characteristic drop of microtubule density in the central part of the spindle were also observed upon supplementing the extract with $XErp^{ND}$. Under these conditions, APC/C activation was inhibited, and, therefore, securin and cyclin B stayed stable (Fig. 6, A and B; CaMKII* + $XErp^{ND}$). Those partially depolymerized spindle structures were stable for >60 min (unpublished data). Even after elevated times, we did not visualize any spindle structures in which chromosomes had commenced to segregate (Fig. 6 A, CaMKII* + $XErp^{ND}$). As observed for Ran-GTP–mediated microtubule assemblies, anaphase induction by low CaMKII* activity in the presence of cyclinBΔ90 was insufficient to destabilize microtubules and thus revealed spindles with a similar microtubule density distribution but an even higher overall fluorescence than metaphase spindles (Fig. 6 C, compare Meta with low CaMKII*). Still, upon adding low CaMKII* activity, we observed chromosome segregation and degradation of cyclin B after 40 min (Fig. 6 D and not depicted).

To investigate the importance of APC/C activation and the degradation of cyclin B after spindle depolymerization without active APC/C, we first treated preassembled mitotic spindles with CaMKII* in the presence of $XErp^{ND}$ (Fig. 6 A, CaMKII* and $XErp^{ND}$) and chased the anaphase spindles with 1 vol of extract, which had been treated with or without CaMKII* in the absence of $XErp^{ND}$ to fully activate APC/C (Fig. 6 E). In the presence of active APC, cyclin B was degraded, and Cdk1 activity was down-regulated (Fig. 6 E, top). Under these conditions, anaphase spindles completely depolymerized, and long interphase microtubules assembled (Fig. 6 E, bottom).

Collectively, these results clearly show that the conclusions made from Ran-GTP–induced microtubule assemblies are valid for complete spindle structures. Consistently, in both model systems, calcium and CaMKII induce the depolymerization of microtubules in anaphase after the release from CSF arrest independently of the activation of APC/C and thus the degradation of securin and cyclin B and the down-regulation of Cdk1.

Discussion

Xenopus egg extracts faithfully recapitulate cell cycle progression and cell cycle–specific reorganization of the microtubule cytoskeleton (e.g., at M-phase entry or at metaphase to anaphase transition). They enter anaphase after CaMKII activation and subsequent degradation of the APC/C inhibitor XErp, which allows chromosome segregation. The initiation of chromosome movement is coupled to a generally reduced stability of spindle microtubules, suggesting a global change in microtubule dynamics parameters. In this study, we used Ran-GTP–induced microtubule assemblies as a straightforward tool to analyze the signal, which is responsible for triggering reduced microtubule stability in anaphase of *Xenopus* egg extracts. Indeed, although the addition of Ran-GTP was sufficient to promote microtubule assemblies in metaphase as expected, no microtubule assemblies

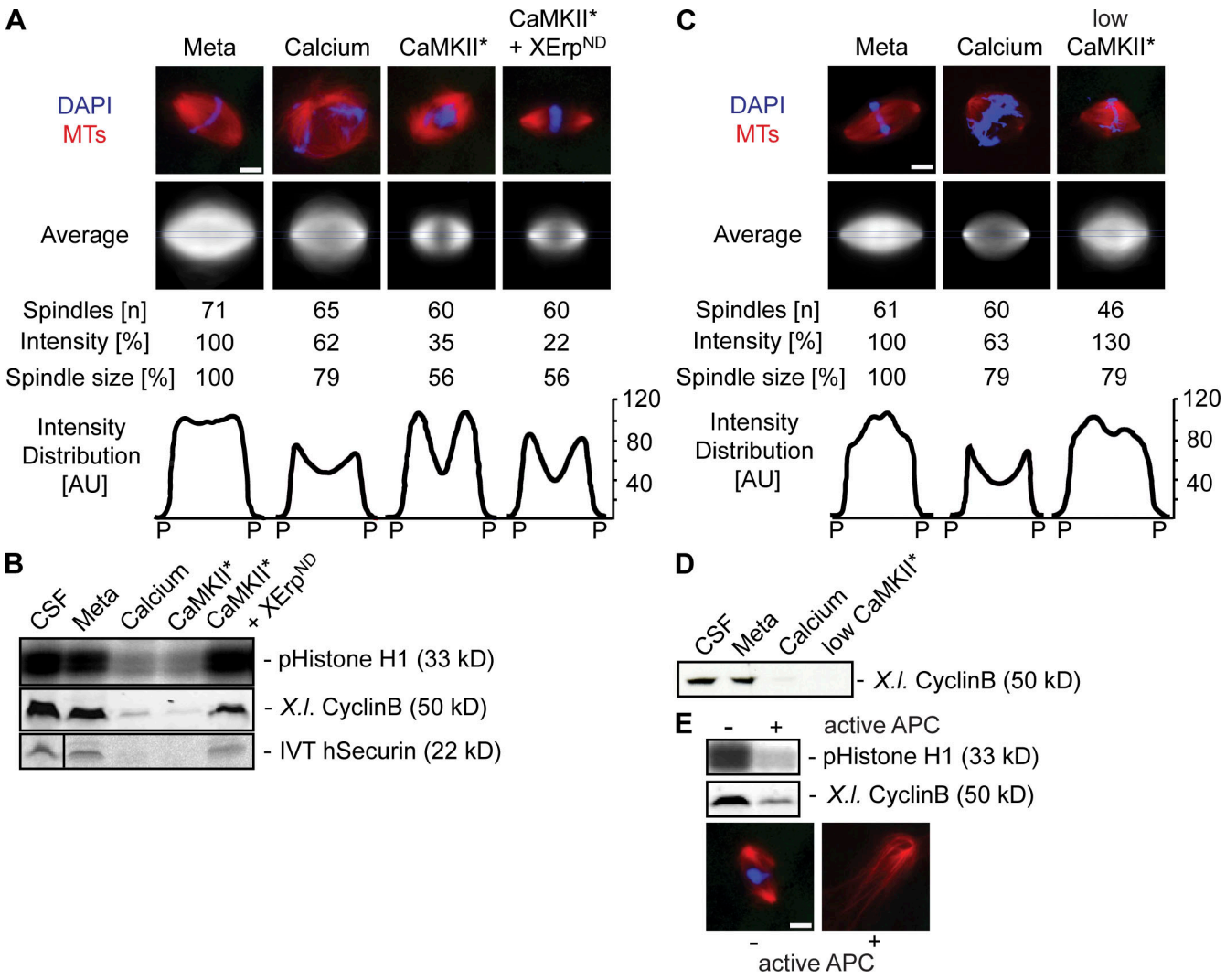

Figure 6. **CaMKII triggers spindle disassembly in anaphase independently of APC/C activation.** Spindles were preassembled in CSF extracts (Meta), and anaphase was induced by the addition of calcium or CaMKII* in the absence or presence of XErpND. (A) Spindles were visualized by direct fluorescence of Cy3-tubulin (red) and DAPI (blue) after 20 min. Out of *n* imaged spindles, the mean overall fluorescence intensity was determined, and an average image was generated using the Matlab macro. The pole (P) to pole distance (spindle size) was measured as well as the corresponding mean fluorescence distribution plotted along the pole to pole axis in a 1.5-µm-wide area (intensity distribution; see blue lines in average images). Intensity and spindle size are indicated in relative terms (percentage). (B) Immunoblots were used to determine the amounts of cyclin B, an autoradiograph was used to monitor amounts of exogenously added in vitro translated (IVT) securin, and an autoradiograph displaying a histone H1 kinase assay was used to determine Cdk1 activity under the conditions used in A. The black line indicates that intervening lanes have been spliced out. (C) Anaphase was induced in preassembled spindles by low doses of CaMKII* in the presence of cyclinBΔ90, and samples were fixed after 40 min. Spindles were analyzed as in A. (D) Determination of cyclin B by immunoblotting under the conditions used in C. (E) Spindles were first treated with CaMKII* and XErpND and mixed with extracts treated without (−) or with (+) CaMKII* to activate APC/C. (top) Immunoblotting was used to determine the amounts of cyclin B and histone H1 kinase assay to measure the Cdk1 activity. (bottom) Representative fluorescence images of structures after 40 min. Tubulin, red; DAPI (DNA), blue. MT, microtubules; Meta, extracts after spindle assembly. Bars, 5 µm.

could be observed upon Ran-GTP addition in anaphase. In the past, assays using Ran-GTP–induced microtubule assemblies led to the identification of molecular mechanisms, which were subsequently confirmed in spindle assembly pathways (Gruss et al., 2001; Blower et al., 2005; Koffa et al., 2006). Likewise, our conclusions suggested from Ran-GTP–mediated microtubule assemblies were consistent with the results from microtubules nucleated by centrosomes and from complete spindles. Collectively, this clearly supports the idea of a global change in microtubule stability, which affects the Ran-GTP–dependent microtubule assembly pathway as well as centrosome-driven microtubule polymerization.

We could show further that Ran-induced microtubule assemblies are destabilized in response to calcium and CaMKII, whereas APC/C activation is not required for this destabilization. Thus, neither degradation of cyclin B nor of securin can be causative for changes in microtubule stability at anaphase onset. Similarly, our experiments in complete spindles show that reduced microtubule stability in anaphase is independent of the inactivation of Cdk1 but is triggered by CaMKII activity; we observed reduced microtubule density in the central part of the spindle upon CaMKII activation even though nondegradable XErp inhibited the APC/C and, therefore, degradation of cyclin B and securin. This is consistent with previous data suggesting

that inactivation of Cdk1 is not necessary to induce anaphase in *Xenopus* egg extracts (Holloway et al., 1993; Murray et al., 1996). It also implies that the decrease in spindle microtubule density in anaphase is not directly influenced by the cohesion state of chromatin because inhibition of APC/C prevents sister chromatid separation but not microtubule destabilization. This is confirmed by our Ran-GTP experiments in which microtubules can only be destabilized in anaphase independently of chromatin structures. Consistent with that, previous data has shown that anaphase microtubule depolymerization and cytokinesis can occur independently of chromatin in grasshopper spermatocytes (Zhang and Nicklas, 1995).

Our experiments suggest a two-pathway model for spindle disassembly. The first pathway, which is reflected by the complete disassembly of Ran-mediated microtubule structures or the destabilization of central microtubules in complete spindles, is independent of Cdk1 inactivation but induced by CaMKII. In this study, CaMKII has at least one but potentially more unknown targets. Interestingly, when we tested Ran-GTP–induced microtubule assemblies in *Xenopus* egg extracts, which had already undergone a complete cell cycle, we found that they were completely stable despite the addition of calcium or CaMKII. These extracts had faced a first calcium activation, XErp had been degraded, and the system was rearrested in the next metaphase upon the addition of cyclinBΔ90 (Fig. S5, available at http://www.jcb.org/cgi/content/full/jcb.200807006/DC1). This observation would go along with conclusions from mitosis in human somatic cells in which CaMKII has a stabilizing effect on spindle microtubules (Holmfeldt et al., 2005). It might also suggest that additional CaMKII targets similar to XErp are inactivated after the first rise in calcium and are not functional anymore in the first mitotic cell cycle.

The second pathway of spindle disassembly requires inactivation of Cdk1, which allows further pole separation and finally complete spindle disassembly and return to interphase (Fig. 6 E; Murray et al., 1989, 1996; Holloway et al., 1993). In *Xenopus* egg extracts, CaMKII is required for the second mechanism because Cdk1 inactivation depends on the activation of APC/C, which in turn requires the CaMKII-induced degradation of XErp. Upon increasing calcium levels, CaMKII will likely activate both pathways in parallel, and those will cooperate to faithfully segregate chromosomes and to disassemble the spindle.

It is almost certain that altered phosphorylation patterns of MAPs or motor proteins are involved in the regulation of both pathways. The fact that there is no change in the phosphorylation of histone H1 in anaphase induced by calcium and cyclinBΔ90 does not preclude the specific activation of counteracting phosphatases on other substrates, and an increased activity of protein phosphatases at anaphase onset might well be required for microtubule destabilization. CaMKII could directly be involved in the activation of protein phosphatases, or, in addition, calcium could trigger phosphatase activation by a different pathway. Mochida and Hunt (2007) and Nishiyama et al. (2007) recently showed that the calcium-calmodulin–dependent phosphatase calcineurin is activated upon rising calcium levels in *Xenopus* eggs and egg extracts and that a second, different phosphatase activity increases subsequently afterward. In our experiments, the addition of cyclosporin A alone to *Xenopus* CSF extracts did not interfere with microtubule depolymerization of Ran-induced structures. However, our observation that calcium addition to CSF-arrested extracts changed the capacity of cyclin B/Cdk1 to partially rescue microtubule stability (Fig. 2) would be consistent with the further activation of protein phosphatases that antagonize the action of Cdk1. We are currently investigating the contribution of different protein phosphatases on anaphase spindle microtubule stability.

What could be the key players directly mediating the changes in microtubule dynamics at anaphase onset? CaMKII action could enhance the activity of microtubule-destabilizing factors or reduce the activity of microtubule-stabilizing proteins and therefore allow more efficient microtubule depolymerization. However, previous experiments of Morin et al. (1994) suggest that CaMKII does not target proteins already associated with the metaphase spindle to induce anaphase. This argues against a release of stabilizing activities from spindle microtubules in anaphase. In turn, it might suggest that microtubule-destabilizing proteins or their regulators are recruited upon transition to anaphase and promote microtubule destabilization. A main destabilizing activity in *Xenopus* egg extracts is the kinesin motor protein XKCM1 (Walczak et al., 1996; Tournebize et al., 2000). The activity of XKCM1 increases significantly upon entry into M phase, resulting in a 5–10-fold increase in the catastrophe frequency in metaphase microtubules (Tournebize et al., 2000; Niethammer et al., 2007). Our microtubule dynamics measurements demonstrate that microtubules are even less stable in anaphase than in metaphase. Although lowered rescue frequencies measured in one out of two experiments (Fig. S3) might have contributed to this effect and high deviations in our dynamics measurements also do not allow us to exclude effects on growth and shrinkage rates, we consider it likely that the observed changes in microtubule stability were caused by an approximately twofold further increase in the catastrophe frequency. A higher catastrophe frequency could be caused by rising XKCM1 activity or microtubule affinity, which might be directly or indirectly triggered by CaMKII at metaphase to anaphase transition.

Collectively, our data put forward the idea that analogous to entry into M phase, a global switch in microtubule dynamics in anaphase is required to cope with the functions of microtubules in chromosome segregation and their subsequent rearrangement upon mitotic exit. These changes in microtubule dynamics are not just caused by immediately declining Cdk1 activity but are, before this, triggered by the CaMKII-dependent phosphorylation of yet unknown substrates.

The key question in the future will therefore be to determine which microtubule-binding activities are possibly meiosis-specific targets of CaMKII in the transition from metaphase to anaphase in *Xenopus* egg extracts. Functional assays at defined conditions using purified CaMKII* and $XErp^{ND}$ might help to identify these activities, to understand how they are modified and modulated at the molecular level, and to understand how their regulation is integrated into global changes in microtubule stability.

Materials and methods

Preparation of *Xenopus* egg extracts, sperm nuclei, chromatin beads, and functional assays in *Xenopus* egg extracts

CSF-arrested (M phase) *Xenopus* egg extracts were prepared as described previously (Murray, 1991; extracts were also provided by K. Ribbeck [Harvard University, Cambridge, MA], C. Casanova [University Hospital of Freiburg, Freiburg, Germany], H. Yokoyama [European Molecular Biology Laboratory, Heidelberg, Germany], S. Rybina [European Molecular Biology Laboratory, Heidelberg, Germany], and W. Antonin [Max Planck Institute for Developmental Biology, Tübingen, Germany]). To obtain anaphase, M-phase extracts were incubated for 40 min at 20°C with cyclinBΔ90 (Stemmann et al., 2001; provided by O. Stemmann [University of Bayreuth, Bayreuth, Germany] and P. Bieling [European Molecular Biology Laboratory, Heidelberg, Germany]), 0.1 mg/ml cycloheximide, and 0.6 mM calcium. Spindle assembly was monitored by adding either 300–500 nuclei/µl of sperm nuclei (Philpott et al., 1991) or chromatin beads (Heald et al., 1996) and 0.2 mg/ml Cy3-labeled tubulin (Hyman et al., 1991) to CSF extract; a full cell cycle was allowed, and the system was rearrested in M phase using CSF extract as described previously (Sawin and Mitchison, 1991; Heald et al., 1996). To assay mitotic microtubule assembly (Fig. S5) at metaphase to anaphase transition, CSF extracts were activated and incubated for 60 min to reach interphase. The addition of cyclinBΔ90 and further incubation for 40 min reestablished metaphase in which RanQ69L-GTP–induced microtubule assemblies could be visualized. Microtubule structures were visualized in squash fixed samples (Heald et al., 1996) except asters assembled from purified human centrosomes (Tournier et al., 1991), which were spun on coverslips (Carazo-Salas et al., 2001). Cdk1 activity was assayed as described previously (Félix et al., 1990).

Data acquisition

To quantify Ran-GTP–induced microtubule assemblies, in each individual experiment at least 500 separate nucleation foci were counted in metaphase controls or after the addition of low CaMKII activity either from 8–10 randomly chosen fields or complete coverslips. The number of structures in the same sample area of anaphase was determined and plotted relative to controls. Error bars represent SDs from three independent experiments. The overall fluorescence intensity of complete spindles was averaged using ImageJ (National Institutes of Health). A custom Matlab macro (The MathWorks, Inc.) was used to compute mean spindle structures. 40–80 structures from different experiments were imaged randomly. The spindles were aligned vertically after manually marking the poles. Pole to pole distances of all spindles were averaged as a measure for spindle size, and the fluorescence distribution in a 1.5-µm broad area along the pole to pole axis was measured and plotted. Fluorescence images were taken at room temperature on a microscope (DM RXA; Leica) using a 1.25 NA 40× oil or 1.0 NA 63× water immersion objective, a digital camera (ORCA ER; Hamamatsu Photonics), and the Openlab software (PerkinElmer). Photoshop (versions 7.0 and CS3; Adobe) and Illustrator (versions CS2 and CS3; Adobe) were used to generate figures.

Inhibitors

H_2O stocks of CaM inhibitor peptide (myosin light chain kinase peptide; EMD), CaMKII inhibitor peptide ($CaMKII_{281–309}$; EMD), and IINtide (EMD) were used at 0.4 mM (Morin et al., 1994). CGP (in H_2O; Sigma-Aldrich) was used at 0.12 mM. Cyclosporin A (in H_2O; EMD) was used at 1 mM.

Antibodies

The following antibodies were used for immunoblotting: rabbit polyclonal antibody against *Xenopus* cyclin B (1:2,000; provided by O. Stemmann; Max Planck Institute, Martinsried, Germany), a mouse monoclonal antibody against human cyclin B1 (1:2,000; Cell Signaling Technology), and the rabbit polyclonal antibody against aurora A/Eg2 (1:1,000; provided by M. Koffa, Democritus University of Thrace, Alexandroupolis, Greece; Koffa et al., 2006). Immunoprecipitation using antibodies against human TPX2 (Gruss et al., 2001) cross reacting with the *Xenopus* orthologue was performed as described previously (Wittmann et al., 2000). TPX2-associated proteins were eluted with CSF-XB and 1 M KCl, TCA precipitated, washed, and applied to SDS-PAGE and specific proteins detected by immunoblotting.

Preparation of recombinant proteins

His-tagged human cyclinB1Δ90 and RanQ69L were expressed in Sf9 insect cells or *Escherichia coli*, respectively, and purified as described previously (Görlich et al., 1994; Izaurralde et al., 1997; Stemmann et al., 2001). Loading of RanQ69L with GTP was performed as described previously (Weis et al., 1996). Radioactively labeled human securin was generated by in vitro transcription translation in TNT Coupled Reticulocyte Lysate Systems (Promega). N-terminally truncated XErp1 ($XErp^{ND}$) was produced as described previously (Rauh et al., 2005).

CaMKII mutant generation, expression, and activity measurements

CaMKII 1–290 (CaMKII*) was cloned into pQE80 and expressed in *E. coli* BL21 Rosetta. A corresponding catalytically inactive mutant in which lysine 42 was replaced by alanine (K42A; Hanks and Quinn, 1991) was generated using the QuikChange Site-Directed Mutagenesis kit (Agilent Technologies). For both constructs, transformed bacteria were grown at 37°C to an OD_{600} of 0.7 and cooled down to 23°C. After induction of protein expression using 0.3 mM IPTG, bacteria were grown overnight at 23°C. Purification on Talon beads (Clontech Laboratories, Inc.) was performed as described by the manufacturer. The volume activity of CaMKII* was determined to be 0.4 U/µl using myelin basic protein and a defined activity of purified protein kinase A (Sigma-Aldrich) in CSF buffer containing 1 mM ATP (Fig. S1). A final concentration of 0.04 U/µl CaMKII* was used for experiments in *Xenopus* egg extracts, and low CaMKII* activities were <0.006 U/µl.

The activity of CaMKII* in *Xenopus* egg extracts was determined using the CaMKII substrate autocamtide-2 (Jones and Persaud, 1998) with a C-terminal His_6 tag. This peptide was covalently coupled to BSA (Peptide Specialties Laboratories) and immobilized on Dynabeads (Talon; Invitrogen). Reactions were performed in a 3-µl extract aliquot for 3 min in the presence of 5 µCi γ-[^{32}P]ATP and were stopped by chilling on ice and dilution in 10 vol of dilution buffer (100 mM KCl, 20 mM Hepes, pH 7.7, and 50 mM NaF). Beads were washed two times in dilution buffer and were eluted in SDS sample buffer. Signals of phosphorylated proteins were detected using a phosphoimager (F3000; Fujifilm) and the corresponding software (V1.8E image reader and image gauche V3.45; Fujifilm).

Microtubule dynamics measurements

10 µl CSF extracts was supplemented with purified human centrosomes and 0.25 mg/ml (1.5 labeling ratio) Cy3-labeled tubulin. To reduce photobleaching, 0.5 µl of saturated hemoglobin solution and 0.33 µl of antifading mix (13.3 µM catalase, 20.8 µM glucose oxidase, and 0.3 M glucose) were added into the extract. 2.7 µl of the mixture was squashed under 22 × 22–mm coverslips. Time lapses were recorded in 2-s intervals using a microscope (Axiovert 200; Carl Zeiss, Inc.) equipped with a camera (CoolSNAP; Roper Scientific), a 100× Plan Apochromat NA 1.4 oil immersion objective lens, and a long-pass rhodamine filter (Chroma Technology Corp.). The positions of centrosomes and microtubule plus ends were tracked in ImageJ, and these coordinates were used to calculate microtubule length. Finally, plots of changes in microtubule length over time were analyzed with a custom-written Matlab macro to estimate the parameters of microtubule dynamics.

Online supplemental material

Figs. S1 and S2 demonstrate the activity of purified CaMKII* in vitro and in *Xenopus* egg extracts (Fig. S1) and the effects of low amounts of CaMKII* in *Xenopus* egg extracts on APC/C activation and microtubule stability (Fig. S2). Fig. S3 analyzes microtubule stability after the addition of calcium and selective inhibition of endogenous CaMKII or calcineurin. Changes in dynamic instability parameters from metaphase to anaphase were determined in Fig. S4 and Videos 1–4, and the effect of calcium or CaMKII* on mitotic microtubules in *Xenopus* egg extract is shown in Fig. S5. Online supplemental material is available at http://www.jcb.org/cgi/content/full/jcb.200807006/DC1.

We thank Kerstin Hupfeld for excellent technical assistance, Maiwen Caudron and Chaitanya Athale for help with Matlab, and Katahrina Ribbeck, Claudia Casanova, Hideki Yokoyama, Sonia Rybina, Peter Bieling, Wolfram Antonin, and Olaf Stemmann for extracts and other reagents. We are grateful to Jan Ellenberg, Eric Karsenti, and Iain Mattaj for support.

This project was supported by the Deutsche Forschungsgemeinschaft (grant 1737/4-1 and -2 to O.J. Gruss), Fonds der Chemischen Industrie (Kékulé grant to S. Over), and the Zentrum für Molekulare Biologie Heidelberg.

Submitted: 2 July 2008
Accepted: 13 November 2008

References

Blower, M.D., M. Nachury, R. Heald, and K. Weis. 2005. A Rae1-containing ribonucleoprotein complex is required for mitotic spindle assembly. *Cell.* 121:223–234.

Busa, W.B., and R. Nuccitelli. 1985. An elevated free cytosolic Ca2+ wave follows fertilization in eggs of the frog, *Xenopus laevis*. *J. Cell Biol.* 100:1325–1329.

Carazo-Salas, R.E., G. Guarguaglini, O.J. Gruss, A. Segref, E. Karsenti, and I.W. Mattaj. 1999. Generation of GTP-bound Ran by RCC1 is required for chromatin-induced mitotic spindle formation. *Nature.* 400:178–181.

Carazo-Salas, R.E., O.J. Gruss, I.W. Mattaj, and E. Karsenti. 2001. Ran-GTP coordinates regulation of microtubule nucleation and dynamics during mitotic-spindle assembly. *Nat. Cell Biol.* 3:228–234.

Cassimeris, L., and R.V. Skibbens. 2003. Regulated assembly of the mitotic spindle: a perspective from two ends. *Curr. Issues Mol. Biol.* 5:99–112.

Cassimeris, L., and C. Spittle. 2001. Regulation of microtubule-associated proteins. *Int. Rev. Cytol.* 210:163–226.

Chang, B.H., S. Mukherji, and T.R. Soderling. 2001. Calcium/calmodulin-dependent protein kinase II inhibitor protein: localization of isoforms in rat brain. *Neuroscience.* 102:767–777.

Ciciarello, M., R. Mangiacasale, and P. Lavia. 2007. Spatial control of mitosis by the GTPase Ran. *Cell. Mol. Life Sci.* 64:1891–1914.

Clarke, P.R., and C. Zhang. 2004. Spatial and temporal control of nuclear envelope assembly by Ran GTPase. *Symp. Soc. Exp. Biol.* 193–204.

Compton, D.A. 2000. Spindle assembly in animal cells. *Annu. Rev. Biochem.* 69:95–114.

Desai, A., P.S. Maddox, T.J. Mitchison, and E.D. Salmon. 1998. Anaphase A chromosome movement and poleward spindle microtubule flux occur at similar rates in *Xenopus* extract spindles. *J. Cell Biol.* 141:703–713.

Félix, M.A., P. Cohen, and E. Karsenti. 1990. Cdc2 H1 kinase is negatively regulated by a type 2A phosphatase in the *Xenopus* early embryonic cell cycle: evidence from the effects of okadaic acid. *EMBO J.* 9:675–683.

Gadde, S., and R. Heald. 2004. Mechanisms and molecules of the mitotic spindle. *Curr. Biol.* 14:R797–R805.

Görlich, D., S. Prehn, R.A. Laskey, and E. Hartmann. 1994. Isolation of a protein that is essential for the first step of nuclear import. *Cell.* 79:767–778.

Gruss, O.J., and I. Vernos. 2004. The mechanism of spindle assembly: functions of Ran and its target TPX2. *J. Cell Biol.* 166:949–955.

Gruss, O.J., R.E. Carazo-Salas, C.A. Schatz, G. Guarguaglini, J. Kast, M. Wilm, N. Le Bot, I. Vernos, E. Karsenti, and I.W. Mattaj. 2001. Ran induces spindle assembly by reversing the inhibitory effect of importin alpha on TPX2 activity. *Cell.* 104:83–93.

Hanks, S.K., and A.M. Quinn. 1991. Protein kinase catalytic domain sequence database: identification of conserved features of primary structure and classification of family members. *Methods Enzymol.* 200:38–62.

Hansen, D.V., J.J. Tung, and P.K. Jackson. 2006. CaMKII and polo-like kinase 1 sequentially phosphorylate the cytostatic factor Emi2/XErp1 to trigger its destruction and meiotic exit. *Proc. Natl. Acad. Sci. USA.* 103:608–613.

Heald, R., R. Tournebize, T. Blank, R. Sandaltzopoulos, P. Becker, A. Hyman, and E. Karsenti. 1996. Self-organization of microtubules into bipolar spindles around artificial chromosomes in *Xenopus* egg extracts. *Nature.* 382:420–425.

Holloway, S.L., M. Glotzer, R.W. King, and A.W. Murray. 1993. Anaphase is initiated by proteolysis rather than by the inactivation of maturation-promoting factor. *Cell.* 73:1393–1402.

Holmfeldt, P., X. Zhang, S. Stenmark, C.E. Walczak, and M. Gullberg. 2005. CaMKIIgamma-mediated inactivation of the Kin I kinesin MCAK is essential for bipolar spindle formation. *EMBO J.* 24:1256–1266.

Hyman, A., D. Drechsel, D. Kellogg, S. Salser, K. Sawin, P. Steffen, L. Wordeman, and T. Mitchison. 1991. Preparation of modified tubulins. *Methods Enzymol.* 196:478–485.

Izaurralde, E., U. Kutay, C. von Kobbe, I.W. Mattaj, and D. Gorlich. 1997. The asymmetric distribution of the constituents of the Ran system is essential for transport into and out of the nucleus. *EMBO J.* 16:6535–6547.

Jones, P.M., and S.J. Persaud. 1998. Ca(2+)-induced loss of Ca2+/calmodulin-dependent protein kinase II activity in pancreatic beta-cells. *Am. J. Physiol.* 274:E708–E715.

Kline-Smith, S.L., and C.E. Walczak. 2004. Mitotic spindle assembly and chromosome segregation: refocusing on microtubule dynamics. *Mol. Cell.* 15:317–327.

Koffa, M.D., C.M. Casanova, R. Santarella, T. Kocher, M. Wilm, and I.W. Mattaj. 2006. HURP is part of a Ran-dependent complex involved in spindle formation. *Curr. Biol.* 16:743–754.

Liu, J., and J.L. Maller. 2005. Calcium elevation at fertilization coordinates phosphorylation of XErp1/Emi2 by Plx1 and CaMK II to release metaphase arrest by cytostatic factor. *Curr. Biol.* 15:1458–1468.

Lorca, T., F.H. Cruzalegui, D. Fesquet, J.C. Cavadore, J. Mery, A. Means, and M. Doree. 1993. Calmodulin-dependent protein kinase II mediates inactivation of MPF and CSF upon fertilization of *Xenopus* eggs. *Nature.* 366:270–273.

Maddox, P., A. Straight, P. Coughlin, T.J. Mitchison, and E.D. Salmon. 2003. Direct observation of microtubule dynamics at kinetochores in *Xenopus* extract spindles: implications for spindle mechanics. *J. Cell Biol.* 162:377–382.

Mitchison, T.J., and E.D. Salmon. 2001. Mitosis: a history of division. *Nat. Cell Biol.* 3:E17–E21.

Mochida, S., and T. Hunt. 2007. Calcineurin is required to release *Xenopus* egg extracts from meiotic M phase. *Nature.* 449:336–340.

Morin, N., A. Abrieu, T. Lorca, F. Martin, and M. Doree. 1994. The proteolysis-dependent metaphase to anaphase transition: calcium/calmodulin-dependent protein kinase II mediates onset of anaphase in extracts prepared from unfertilized *Xenopus* eggs. *EMBO J.* 13:4343–4352.

Murray, A.W., M.J. Solomon, and M.W. Kirschner. 1989. The role of cyclin synthesis and degradation in the control of maturation promoting factor activity. *Nature.* 339:280–286.

Murray, A.W. 1991. Cell cycle extracts. *Methods Cell Biol.* 36:581–605.

Murray, A.W., A.B. Desai, and E.D. Salmon. 1996. Real time observation of anaphase in vitro. *Proc. Natl. Acad. Sci. USA.* 93:12327–12332.

Nasmyth, K. 2002. Segregating sister genomes: the molecular biology of chromosome separation. *Science.* 297:559–565.

Niethammer, P., I. Kronja, S. Kandels-Lewis, S. Rybina, P. Bastiaens, and E. Karsenti. 2007. Discrete states of a protein interaction network govern interphase and mitotic microtubule dynamics. *PLoS Biol.* 5:e29.

Nishiyama, T., N. Yoshizaki, T. Kishimoto, and K. Ohsumi. 2007. Transient activation of calcineurin is essential to initiate embryonic development in *Xenopus laevis*. *Nature.* 449:341–345.

Philpott, A., G.H. Leno, and R.A. Laskey. 1991. Sperm decondensation in *Xenopus* egg cytoplasm is mediated by nucleoplasmin. *Cell.* 65:569–578.

Rauh, N.R., A. Schmidt, J. Bormann, E.A. Nigg, and T.U. Mayer. 2005. Calcium triggers exit from meiosis II by targeting the APC/C inhibitor XErp1 for degradation. *Nature.* 437:1048–1052.

Sawin, K.E., and T.J. Mitchison. 1991. Mitotic spindle assembly by two different pathways in vitro. *J. Cell Biol.* 112:925–940.

Schmidt, A., P.I. Duncan, N.R. Rauh, G. Sauer, A.M. Fry, E.A. Nigg, and T.U. Mayer. 2005. *Xenopus* polo-like kinase Plx1 regulates XErp1, a novel inhibitor of APC/C activity. *Genes Dev.* 19:502–513.

Skoufias, D.A., R.L. Indorato, F. Lacroix, A. Panopoulos, and R.L. Margolis. 2007. Mitosis persists in the absence of Cdk1 activity when proteolysis or protein phosphatase activity is suppressed. *J. Cell Biol.* 179:671–685.

Stemmann, O., H. Zou, S.A. Gerber, S.P. Gygi, and M.W. Kirschner. 2001. Dual inhibition of sister chromatid separation at metaphase. *Cell.* 107:715–726.

Tournebize, R., A. Popov, K. Kinoshita, A.J. Ashford, S. Rybina, A. Pozniakovsky, T.U. Mayer, C.E. Walczak, E. Karsenti, and A.A. Hyman. 2000. Control of microtubule dynamics by the antagonistic activities of XMAP215 and XKCM1 in *Xenopus* egg extracts. *Nat. Cell Biol.* 2:13–19.

Tournier, F., M. Cyrklaff, E. Karsenti, and M. Bornens. 1991. Centrosomes competent for parthenogenesis in *Xenopus* eggs support procentriole budding in cell-free extracts. *Proc. Natl. Acad. Sci. USA.* 88:9929–9933.

Tung, J.J., D.V. Hansen, K.H. Ban, A.V. Loktev, M.K. Summers, J.R. Adler III, and P.K. Jackson. 2005. A role for the anaphase-promoting complex inhibitor Emi2/XErp1, a homolog of early mitotic inhibitor 1, in cytostatic factor arrest of *Xenopus* eggs. *Proc. Natl. Acad. Sci. USA.* 102:4318–4323.

Verde, F., J.C. Labbé, M. Dorée, and E. Karsenti. 1990. Regulation of microtubule dynamics by cdc2 protein kinase in cell-free extracts of *Xenopus* eggs. *Nature.* 343:233–238.

Walczak, C.E., T.J. Mitchison, and A. Desai. 1996. XKCM1: a *Xenopus* kinesin-related protein that regulates microtubule dynamics during mitotic spindle assembly. *Cell.* 84:37–47.

Weis, K., C. Dingwall, and A.I. Lamond. 1996. Characterization of the nuclear protein import mechanism using Ran mutants with altered nucleotide binding specificities. *EMBO J.* 15:7120–7128.

Wittmann, T., M. Wilm, E. Karsenti, and I. Vernos. 2000. TPX2, a novel *Xenopus* MAP involved in spindle pole organization. *J. Cell Biol.* 149:1405–1418.

Wittmann, T., A. Hyman, and A. Desai. 2001. The spindle: a dynamic assembly of microtubules and motors. *Nat. Cell Biol.* 3:E28–E34.

Yanagida, M. 2005. Basic mechanism of eukaryotic chromosome segregation. *Philos. Trans. R. Soc. Lond. B Biol. Sci.* 360:609–621.

Zhang, D., and R.B. Nicklas. 1995. Chromosomes initiate spindle assembly upon experimental dissolution of the nuclear envelope in grasshopper spermatocytes. *J. Cell Biol.* 131:1125–1131.